

Phase equilibria in stratified thin liquid films stabilized by colloidal particles

J. BLAWZDZIEWICZ¹ AND E. WAJNRYB^{1,2}

¹ Department of Mechanical Engineering, Yale University, P.O. Box 20-8286, New Haven, CT 06520, U.S.A.

² On leave from IPPT Warsaw, Poland.

PACS. 68.15.+e – Liquid thin films.

PACS. 68.18.Jk – Phase transitions.

PACS. 82.70.Dd – Colloids.

Abstract. –

Phase equilibria between regions of different thickness in thin liquid films stabilized by colloidal particles are investigated using a quasi-two-dimensional thermodynamic formalism. Appropriate equilibrium conditions for the film tension, normal pressure, and chemical potential of the particles in the film are formulated, and it is shown that the relaxation of these parameters occurs consecutively on three distinct time scales. Film stratification is described quantitatively for a hard-sphere suspension using a Monte-Carlo method to evaluate thermodynamic equations of state. Coexisting phases are determined for systems in constrained- and full-equilibrium states that correspond to different stages of film relaxation.

Drainage of thin liquid films often involves spontaneous formation of coexisting regions of different, but uniform, thickness. For example, circular black-film spots can be seen in soap bubbles prior to breakup. Such a stratification phenomenon is particularly interesting in films stabilized by colloidal particles, micelles, or polyelectrolytes, where the thinning occurs through a series of stepwise transitions between film states characterized by the thickness commensurate with the size of the stabilizing particles. In experiments with horizontal films [1, 2], such transitions occur by rapid formation of circular regions of a smaller thickness, followed by a much slower expansion. In investigations of vertical films, up to seven coexisting parallel stripes of different thickness have been observed [3].

Film stratification has recently been intensively studied [1–8] because of the relevance of the problem for understanding structural colloidal forces. In particle-stabilized thin liquid films, the structural forces depend on the film thickness in an oscillatory manner due to particle layering [9]. Equilibrium values of the film thickness result from the balance between the normal pressure in the film (which includes the oscillatory structural force) and the outside pressure [6, 7, 10]. We find, however, that the normal-stress balance used alone in descriptions of the film stratification phenomenon is insufficient—the mechanical equilibrium between regions (phases) of different thickness requires also the lateral force balance. Since the lateral balance has not been included in the available theories, understanding of an essential aspect of

the problem is still lacking. One of our goals is to provide a proper thermodynamic framework for analyzing the phase behavior of particle stabilized thin liquid films.

An analysis of the stepwise-thinning phenomenon requires equilibrium as well as nonequilibrium considerations. Experimental observations indicate that the thinning process occurs on several distinct time scales: a thinner spot nucleates in a fraction of a second but the time scale for the subsequent expansion of the spot is much slower. This separation of the time scales suggests that the system at different evolution stages is, approximately, in *constrained equilibrium*. In such states the film phases of uniform thickness are in equilibrium. However, only some of the equilibrium conditions between these phases are satisfied—the others are not, due to dynamical constraints. An important goal of our study is to identify relevant time scales in the stepwise-thinning phenomenon, and to discern the corresponding relaxation processes. Our theoretical considerations are supplemented with results of Monte-Carlo simulations of a model system to illustrate possible full and partial equilibrium states of a stratified particle-stabilized film at different evolution stages.

Our analysis of the film stratification phenomenon relies on representing the film as an effective two-dimensional medium [9, 11]. Accordingly, all details of the transverse structure of the film are averaged out (as in the thermodynamic description of an interface proposed by Gibbs). The film thickness, however, is retained as a parameter of state, because it can be controlled by varying the difference between the external pressure $p^{(e)}$ and the pressure of the bulk fluid in contact with the fluid in the film. We note that the usual formulation of thin-film thermodynamics [9] is insufficient for our problem because of the underlying assumptions that the pressure in the film is isotropic and the interaction between the film interfaces is described by a mean-field normal force. In contrast, the stabilizing colloidal particles contribute not only to the normal but also to the tangential stress balance in the film, and the corresponding stress tensor is non-isotropic due to confinement effects. These features have to be taken into account in the proper formulation of the theory.

A typical thickness of a particle-stabilized liquid film is in the micrometer range, consistent with the size of colloidal particles. On this scale, the film interfaces can be treated as surfaces with zero thickness and interfacial tension σ . Assuming this geometry, a suitable effective two-dimensional thermodynamic description can be obtained from the expression for the macroscopic infinitesimal work

$$dW = -Ap_{\perp} dh + (2\sigma - h\bar{p}_{\parallel}) dA \quad (1)$$

associated with changes of the film thickness h and area A . In the above relation, p_{\perp} and p_{\parallel} denote the normal and lateral components of the pressure tensor in the film and the overbar indicates the average value across the film. If a direct interaction force (*e.g.*, the van der Waals attraction or electrostatic repulsion) acts between the film interfaces, the normal pressure p_{\perp} in eq. (1) should be replaced with $p_{\perp} + f_n$, where f_n is the normal force per unit area, and $f_n > 0$ corresponds to attraction.

In eq. (1), the work associated with the area change consists of the interfacial-tension and pressure contributions. To obtain an effective two-dimensional thermodynamic description of the film, the lateral interfacial-tension forces and the pressure are combined into a single conjugate thermodynamic variable. However, first an appropriate set of independent thermodynamic parameters has to be chosen. The pair of independent variables h and A used in Eq. (1) is unsuitable because h is not an extensive quantity. By a simple change of variables, a more appropriate form is obtained

$$dW = -p_{\perp} dV + \gamma dA, \quad (2)$$

where $V = Ah$ is the film volume, and, by analogy with the definition of the surface tension,

$$\gamma = h(p_{\perp} - \bar{p}_{\parallel}) + 2\sigma \quad (3)$$

is the tension of the film [11].

The fundamental relation for the film free energy F can be derived in the usual way from the expression for mechanical work (2). Treating the suspension in the film as a two-component fluid (with the colloidal particles regarded as macromolecules) we get

$$dF = -S dT - p_{\perp} dV + \gamma dA, + \mu_c dN_c + \mu_f dN_f, \quad (4)$$

where N_c and N_f denote the number of colloidal particles and solvent molecules in the system, and μ_c and μ_f are the corresponding chemical potentials. The film-tension representation (4) of the film free energy is more suitable for discussion of phase equilibria in stratified films than the more common film surface tension representation where the film thickness h is retained as an independent thermodynamic parameter. Since all independent parameters in our representation V, A, N_c and N_f are extensive, the conjugate intensive functions of state p_{\perp}, γ, μ_c , and μ_f in coexisting phases must be equal in unconstrained equilibrium (which follows from standard entropy-maximization arguments [12]). Accordingly, apart from the trivial thermal-equilibrium condition $T^{(1)} = T^{(2)} = T^{(e)}$, there are the transverse and lateral mechanical equilibrium conditions

$$p_{\perp}^{(1)} = p_{\perp}^{(2)} = p^{(e)}, \quad \gamma^{(1)} = \gamma^{(2)}, \quad (5a,b)$$

and the chemical equilibrium conditions

$$\mu_c^{(1)} = \mu_c^{(2)}, \quad \mu_f^{(1)} = \mu_f^{(2)}, \quad (6a,b)$$

where $T^{(e)}$ and $p^{(e)}$ are the external temperature and pressure.

A typical size of colloidal particles used in experiments with stratified thin films (or the range of the effective screened Coulombic potential if the particles are charged) is $\gtrsim 0.1 \mu\text{m}$. Under these conditions the solvent can be treated as a structureless incompressible continuous medium that does not affect thermodynamic properties of the system. In our further considerations the solvent variables μ_f and N_f are thus neglected (which is a usual approximation), and the equilibrium conditions (5) are rephrased in terms of the excess quantities associated with the particle presence,

$$p_{c\perp}^{(1)} = p_{c\perp}^{(2)}, \quad \gamma_c^{(1)} = \gamma_c^{(2)}, \quad (7a,b)$$

where the index c indicates the particle contributions.

As demonstrated in numerous experiments, formation of a stepwise structure in particle-stabilized films is much faster than the subsequent evolution of the coexisting phases [1–3]. Scaling arguments, outlined below, suggest that the relaxation of a stratified film is characterized by three distinct time scales $\tau_{\parallel} \ll \tau_{\perp} \ll \tau_c$ for attaining the equilibrium conditions (7b), (7a), and (6a), respectively. The corresponding nonequilibrium thermodynamic processes entail changes in the areas of individual phases, their volumes, and the volume fraction of colloidal particles.

Estimates of the characteristic relaxation times can be obtained using energy-dissipation arguments. To evaluate the time scale τ_{\parallel} we note that the area change involves energy dissipation in the whole volume of the film V and is characterized by the velocity variation on the lengthscale l set by the lateral film dimension. By comparing the energy-dissipation rate $V\eta(u/l)^2$ to the power $ulhnckT$ associated with the thermal stresses n_ckT produced by the particles, we find $\tau_{\parallel} \sim \eta/n_ckT$, where η is the fluid viscosity, $u \sim l/\tau_{\parallel}$ is the characteristic film velocity, $n_c = N_c/V$, and kT is the thermal energy. The change in the volume of the coexisting phases requires suspension flow through the contact region where the film thickness changes

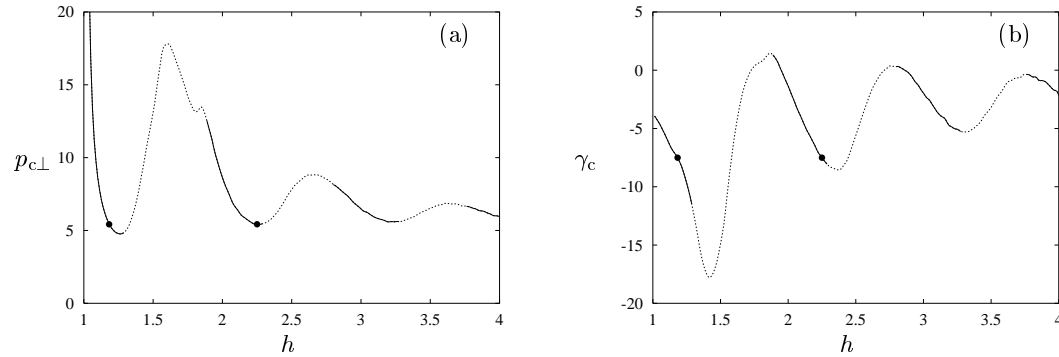


Fig. 1 – Particle contribution to normal pressure $p_{c\perp}$ and film tension γ_c versus film thickness h for particle volume fraction $\phi_c = 0.4$. Dotted lines correspond to states for which the stability condition (10) is violated. Circles indicate a pair of stable phases in mechanical equilibrium (7).

rapidly. Accordingly, the magnitude of the velocity gradient is $O(u/h)$ and the dissipation occurs in the volume $(h/l)V$, which yields the estimate $\tau_\perp \sim (l/h)\tau_\parallel$. A change of the particle volume fraction ϕ_c involves particle motion with respect to the fluid in the whole volume of the film. Assuming $d \sim h$ (where d is the particle diameter) and $\phi_c = O(1)$ we find that $\tau_c \sim (l/h)\tau_\perp$. For an aqueous suspension of particles with the diameter $d = 0.1 \mu\text{m}$ in a film with the characteristic lateral dimension $l = 10 \mu\text{m}$ we find $\tau_\parallel \sim 10^{-3} \text{ s}$, $\tau_\perp \sim 10^{-1} \text{ s}$, and $\tau_c \sim 10 \text{ s}$, which is consistent with experimental observations [2]. We note that our scaling analysis applies to films with surfactant-free interfaces (as in the experiments reported in [2]). We expect that a surfactant adsorbed on film interfaces may increase the time scale τ_\perp by a factor l/h , due to the modification of hydrodynamic boundary conditions. Also, the timescale τ_c may be decreased by a factor d/h for charged particles with $d \ll h$.

Assuming the separation of time scales $\tau_\parallel \ll \tau_\perp \ll \tau_c$ we anticipate the following scenario for the stepwise-thinning of the film. At an early stage of phase separation, the relaxation occurs on the time scale τ_\parallel primarily through a change in the areas of the coexisting phases at constant ϕ_c . The process is driven by an imbalance of lateral forces, and after it is completed the film is in a constrained equilibrium state where only the lateral-force equilibrium condition (7b) between the coexisting phases is satisfied. (An analogy is the coexistence of water and air where the pressure difference between the two phases relaxes very fast, but equilibration of the temperature and chemical-potential differences is much slower.) The next stage of the film evolution is driven by the difference $\Delta p_{c\perp}$ of the colloidal contribution to the normal pressure in the coexisting regions. As required by the incompressibility of the suspension in the film, this pressure difference is compensated by the dynamic pressure drop due to the suspension flow through the contact region. After the pressure difference $\Delta p_{c\perp}$ has relaxed on the time scale τ_\perp the chemical potential of colloidal particles relaxes on the time-scale τ_c due to the particle diffusion in the film. Only this last process entails a change of particle volume fraction in the coexisting regions.

Our theory can be used to obtain quantitative predictions for the trajectory in the thermodynamic parameter space for a stratified film during the equilibration process. To this end the general thermodynamic relations have to be supplemented with equilibrium equations of state. We present numerical results for a film stabilized by a monodisperse suspension of

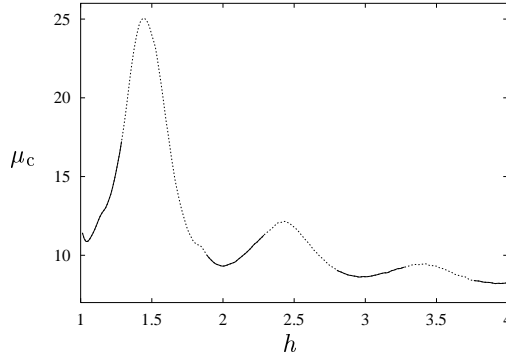


Fig. 2 – Chemical potential of the particles μ_c versus film thickness h for $\phi_c = 0.4$. The normalization corresponds to the asymptotic behavior $\mu_c = -\ln v$ for $\phi_c \ll 1$. Dotted line as in fig. 1.

hard spheres. The particle contribution to average stress tensor \bar{p}_c in homogeneous phases is evaluated from the contact value of the equilibrium two-particle density $n_2^{\text{eq}}(\mathbf{r}_1, \mathbf{r}_2)$ in the confined suspension using the relation

$$\frac{\bar{p}_c}{kT} = n'_c + \frac{1}{2}d^3 \left\langle \int \hat{\mathbf{r}} \hat{\mathbf{r}} n_2^{\text{eq}}(\mathbf{r}_1, \mathbf{r}_1 - d\hat{\mathbf{r}}) d^2\hat{\mathbf{r}} \right\rangle_{V'} . \quad (8)$$

Here $\hat{\mathbf{r}} = \mathbf{r}/r$, the integration is over the contact configurations, $\langle \dots \rangle_{V'}$ denotes the volume average over the region $V' = A(h - d)$ accessible to particle centers, and $n'_c = N_c/V'$ is the corresponding particle number density⁽¹⁾. Equation (8) generalizes a well-known expression for the pressure in a bulk hard-sphere system in terms of the contact value of the radial distribution. It can be derived either from the collisional contribution to the momentum flux or by passing to the hard-sphere limit of the Kirkwood-Buff expression [13] for the stress tensor in an inhomogeneous fluid. The equilibrium average involved in (8) was evaluated via computer simulations using the standard Metropolis algorithm to generate the canonical ensemble for a system of several hundred spheres confined in a planar film with periodic boundary conditions in the lateral directions.

A typical dependence of the normal pressure $p_{c\perp}$ and film tension γ_c on the film thickness h at a constant volume fraction ϕ_c is shown in fig. 1. By integrating the Gibbs-Duhem relation at fixed T

$$d\mu_c = v dp_{c\perp} - a d\gamma_c \quad (9)$$

(where $v = V/N_c$ and $a = A/N_c$), we also determined the chemical potential μ_c . The plot of μ_c versus h at constant ϕ_c is presented in fig. 2. The film thickness h is normalized here by the particle diameter d , pressure $p_{c\perp}$ by kT/d^3 , film tension γ_c by kT/d^2 , and chemical potential μ_c by kT . As expected, the intensive parameters $p_{c\perp}$, γ_c , and μ_c oscillate as functions of the film thickness h . Simulation results at different volume fractions (not shown) indicate that the oscillations are more pronounced at higher ϕ_c . We note that the thermodynamic stability of the system requires that

$$(\partial p_{c\perp}/\partial h)_{T\mu_c} < 0, \quad (10)$$

⁽¹⁾The accessible volume V' rather than the total volume V appears in eq. (8) because \bar{p}_c is the average of the local stress tensor $p_c(\mathbf{r})$ that vanishes for $\mathbf{r} \notin V'$. Consistently, we use the relation $\gamma_c = h'(\bar{p}_{c\parallel} - \bar{p}_{c\perp})$ for the particle contribution to the film tension.

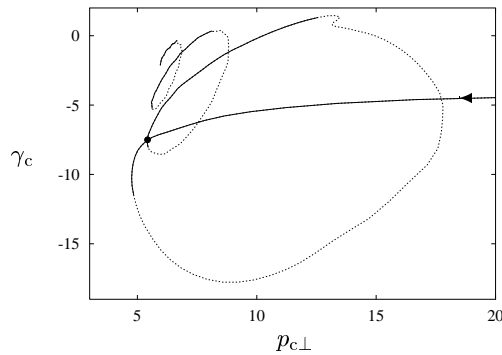


Fig. 3

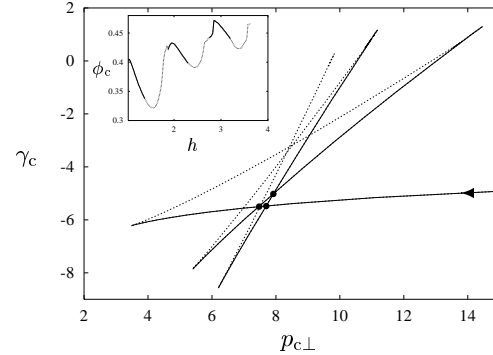


Fig. 4

Fig. 3 – Parametric plot of the equation of state in the $(p_{c\perp}, \gamma_c)$ plane at constant particle volume fraction $\phi_c = 0.4$. The curve is parametrized by film thickness h ; direction of the increasing h is indicated by the arrow. Dotted line as in fig. 1. Circle indicates the stable coexistence state.

Fig. 4 – Same as fig. 3, except that the results are for the constant chemical potential $\mu_c = 11$. Inset shows the variation of the particle volume fraction with the film thickness h along the curve. Circles indicate stable coexistence states; film thickness in the coexisting phases is $(h_1, h_2) = (1.1, 3.0)$, $(1.1, 2.1)$, and $(2.0, 3.0)$.

which is equivalent to $(\partial \gamma_c / \partial h)_{T\mu_c} < 0$. The domains where (10) is violated are indicated in the figures by dotted lines.

We now return to our discussion of phase equilibria at different stages of film evolution. As predicted by our scaling analysis, the first two stages occur at a constant volume fraction $\phi_c^{(1)} = \phi_c^{(2)}$. At the end of the first stage, the coexisting phases fulfill the lateral mechanical-equilibrium condition (7b); accordingly, the film thickness in these phases satisfies equation $\gamma_c(h) = \gamma_0$, where the film tension is evaluated at constant ϕ_c , as in fig. 1b. The value of the constant γ_0 is not determined by the equilibrium condition (7b) alone, but it also depends on the initial volumes of the coexisting regions. The oscillatory character of the curve $\gamma_c = \gamma_c(h)$ in fig. 1b indicates that several different combinations of coexisting phases are possible.

At the next relaxation stage, the complete mechanical equilibrium is attained. Since two equilibrium conditions (7) are now satisfied, the coexisting phases correspond to isolated points in the space of states for given ϕ_c . The coexisting phases can be determined from the equations of state $p_{c\perp} = p_{c\perp}(h)$ and $\gamma_c = \gamma_c(h)$ by combining them into a single parametric plot, as shown in fig. 3 for $\phi_c = 0.4$. The coexisting phases correspond to the line intersections. In our example only one intersection (indicated by the circle) represents a stable system. The two coexisting phases are also marked in fig. 1. Additional numerical calculations show that at higher volume fractions several distinct stable states with coexisting phases can be identified, and for lower ϕ_c there are no such states. We emphasize that not only do the intersection points in fig. 3 have a physical meaning but also the curve itself does—its different portions represent the trajectory of the system in the space of states when the normal-pressure difference relaxes.

A similar parametric plot can be used to determine the possible coexisting phases in full thermodynamic equilibrium. However, the chemical potential μ_c is now held constant, instead of ϕ_c , due to the equilibrium condition (6a). An example of such a plot is presented in fig. 4; the inset shows the corresponding variation of the volume fraction ϕ_c with the film thickness

h . The shape of the curve $\mu_c = \text{const}$ in the $(p_{c\perp}, \gamma_c)$ plane is entirely different from the shape of the line $\phi_c = \text{const}$ in fig. 3. The distinct qualitative features of the curve plotted in fig. 4 follow from Frumkin [14] equation $(\partial\gamma_c/\partial p_{c\perp})_{T\mu_c} = h$ (which can be derived from (9)). Frumkin equation implies that the slope of the line $\gamma_c = \gamma_c(p_{c\perp})$ at constant μ_c is always positive and grows with the increasing h . Moreover, the extrema of the functions $p_{c\perp}(h)$ and $\gamma_c(h)$ at constant μ_c coincide, which causes the sharp corners in the plot.

The line $\gamma_c = \gamma_c(p_{c\perp})$ in fig. 4 has numerous intersections, indicating a number of possible combinations of coexisting phases. In contrast, the results in fig. 3 have only one intersection. For a given system several equilibrium states may thus exist, but it may be difficult to reach them in a stepwise-drainage process because of a bottleneck at the second relaxation stage: the evolving coexisting phases may encounter an instability before mechanical equilibrium (7) is reached. After one or more of such transitions the film may break rather than achieve a stable unconstrained-equilibrium configuration. (Indeed, film breakup was observed in most experiments with particle-stabilized films; see, however, recent results reported in [2].)

Designing experiments that would clearly distinguish between different evolution phases of the stepwise-drainage process is a challenge that requires further numerical and theoretical studies. Our approach will be used in our forthcoming study to propose experimental protocols for reaching full equilibrium states predicted by our analysis.

* * *

E.W. was supported by NASA grant NAG3-2704 and J.B. was supported by NSF grants CTS-0201131 and cts-s0348175.

REFERENCES

- [1] NIKOLOV A. D. and WASAN D. T., *Langmuir*, **8** (1992) 2985.
- [2] SETHUMADHAVAN G. N., NIKOLOV A. D. and WASAN D. T., *J. Colloid Interface Sci.*, **240** (2001) 105.
- [3] BASHEVA E. S., DANOV K. D. and KRALCHEVSKY P. A., *Langmuir*, **13** (1997) 4342.
- [4] NIKOLOV A. D., WASAN D. T., KRALCHEVSKY P. A. and IVANOV I. B., *Colloids Surf.*, **67** (1992) 139.
- [5] BERGERON V. and RADKE C. J., *Langmuir*, **8** (1992) 3020.
- [6] THÉODOLY O., TAN J. S., OBER R., WILLIAMS C. E. and BERGERON V., *Langmuir*, **17** (2001) 4910.
- [7] STUBENRAUCH C. and KLITZING R. von, *J. Phys.: Condens. Matter*, **15** (2003) R1197.
- [8] BERGERON V., *Curr. Opin. Colloid Interface Sci.*, **4** (1999) 249.
- [9] KRALCHEVSKY P. A., DANOV K. D. and IVANOV I. B., *Foams. Theory, Measurements, and Applications*, edited by PRUD'HOMME R. K. AND KHAN S. A. (ekker, New York) 1996, p. 1.
- [10] TROKHYMCZUK A., HENDERSON D., NIKOLOV A. D. AND WASAN D. T., *Langmuir*, **17** (2001) 4940.
- [11] IKEDA N., KRUSTEV R., AND MÜLLER H.-J., *Adv. Colloid Interface Sci.*, **108** (2004) 273.
- [12] CALLEN H. B., *Thermodynamics and an introduction to thermostatistics* (Wiley, New York) 1985.
- [13] KIRKWOOD J. G. AND BUFF F., *J. Chem. Phys.*, **17** (1949) 338.
- [14] FRUMKIN A. N., *Zh. Phys. Khim. USSR*, **12** (1938) 337.